EFFECT OF POLYVINYLPYRROLIDONE (PVP) COATING ON THE OPTICAL EMISSION OF ZnO MICRORODS GROWN VIA HYDROTHERMAL METHOD

Roland V. Sarmago and Verdad C. Agulto
National Institute of Physics, Condensed Matter Physics Laboratory,
University of the Philippines, Diliman, Quezon City
rsarmago@gmail.com and averdadagulto@gmail.com

ABSTRACT

Coating with polyvinylpyrrolidone (PVP) altered the optical emission of ZnO microrods grown via hydrothermal method. The initially broad defect emission decreased in intensity and was resolved into green and red emission bands after coating. This result suggests that PVP can potentially be used to target particular defect emissions of ZnO.

Keywords: ZnO, hydrothermal method, polymer coating, photoluminescence

INTRODUCTION

With its wide bandgap and large exciton binding energy, zinc oxide (ZnO) can exhibit ultraviolet (UV) emission at room temperature, making it a potential material for UV lasers [1-4]. Aside from UV emission, ZnO can also emit visible emission because of intrinsic and extrinsic crystal defects [5]. This further allows ZnO to be used in other applications such as visible light-emitting devices, energy conversion, and fluorescence labeling [6-8]. The study and control of ZnO emission is thereby useful in the development of wide-ranging applications. Therefore, different post-synthesis treatments are being studied to alter the optical emission of ZnO. Such treatments include annealing [9,10], plasma treatment [11,12], and coating of ZnO surface with surfactants or polymers [13,14]. In this study, ZnO synthesized using hydrothermal method was coated with polyvinylpyrrolidone (PVP). The PVP polymer can chemically adsorb to ZnO surfaces due to its polar structure [15], and the interaction between PVP molecules and the ZnO surface can result to modified optical emission of ZnO. This paper presents the effect of PVP coating on the room-temperature photoluminescence properties of ZnO microrods grown via the hydrothermal method.

METHODOLOGY

ZnO microrods were fabricated using the hydrothermal method. Zinc acetate dihydrate (ZnAc) and hexamethylenetetramine (HMTA) were used as precursors. First, aqueous solutions of ZnAc and HMTA were separately prepared and then mixed together. The ZnAc and HMTA mixture served as the growth solution for the fabrication of ZnO. Glass substrates were submerged at the bottom of the growth solution, then the growth solution was placed in a water bath which was heated to 90°C with a ramp-up time of 30 minutes. This temperature was maintained for 1 hour to grow the ZnO microrods. The microrods that formed in the growth solution deposited on top of the substrates. After 1 hour, the substrates were harvested and subsequently dried in air. For the polymer coating of the samples, an aqueous solution of polyvinylpyrrolidone (PVP, M_w = 10,000) was first prepared. The PVP concentration was 3.2 mM (ZnAc:PVP = 10:8). The substrates with the ZnO microrods were submerged in the PVP solution. Then, the PVP solution was placed in a water bath which was heated to 50°C. After 1 hour, the coated samples were harvested and subsequently dried in air. The as-grown and PVP-coated ZnO samples were characterized using scanning electron microscopy (SEM), x-ray diffraction (XRD), Raman spectroscopy, fourier transform infrared spectroscopy (FTIR), and photoluminescence (PL) spectroscopy.

RESULTS AND DISCUSSION

The ZnO microrods that formed in the hydrothermal growth solution deposited on top of the substrates in random orientations. Figure 1 shows the SEM image and length and diameter distributions of the as-grown ZnO microrods. The inset of the SEM image shows the hexagonal faceting of a microrod. The average length and average diameter of the microrods are (9.8 ± 1.3) μm and (1.6 ± 0.3) μm, respectively. Figure 2 shows the XRD pattern of the as-grown ZnO. The XRD peaks correspond to hexagonal wurtzite ZnO with lattice parameters a = (3.251 ± 0.002) Å and c = (5.201 ± 0.009) Å. The (100) peak has the highest intensity in the XRD pattern because the microrods are essentially horizontal relative to the substrate, exposing mostly the (100) planes. ZnO prefers to grow along the *c*-axis because of the high surface energy of its basal planes, thus the formation of rod structures.

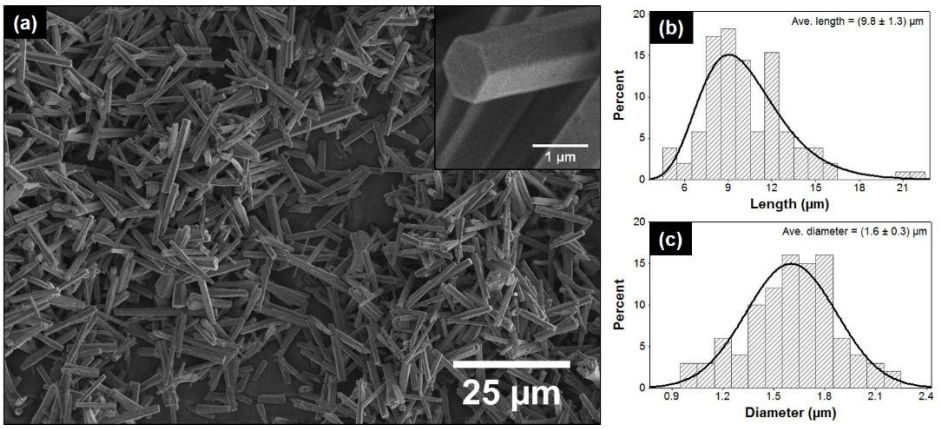

Figure 1. (a) SEM image and (b) length and (c) diameter distributions of as-grown ZnO microrods.

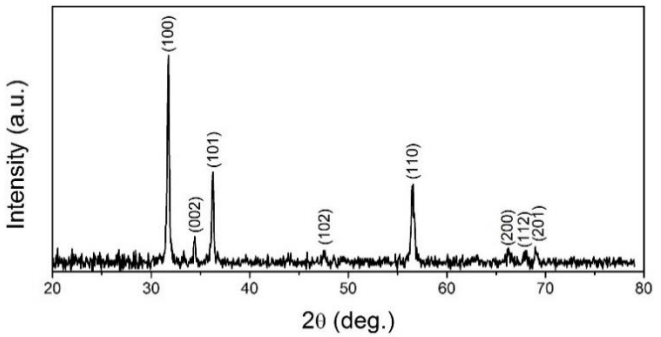

Figure 2. XRD pattern of as-grown ZnO microrods.

Figure 3 shows the room-temperature Raman spectra of the as-grown and PVP-coated ZnO microrods. The Raman peaks in both spectra correspond to first- and second-order Raman scattering in ZnO [16]. The E_2^{high} peak is characteristic of wurtzite ZnO. The Raman spectrum of the PVP-coated ZnO is similar to that of the as-grown ZnO which shows that PVP coating did not affect the ZnO structure. Figure 4 shows the FTIR spectra of PVP, as-grown ZnO and PVP-coated ZnO microrods. The absorbance peaks in the FTIR spectrum of PVP correspond to the intrinsic molecular vibrations in the polymer which are O–H stretching (Peak 1), CH_2 unsymmetrical stretching (Peak 2), C=O stretching (Peak 3), CH_2 bending (Peak 4), and C–N stretching (Peak 5) [17-19]. The as-grown ZnO has O–H stretching band due to adsorbed water, O=C=O vibration (Peak 6) assigned to atmospheric CO_2 absorbed by exposed zinc ions [20], and C–O vibration band (Peak 7) attributed to organic residuals. The PVP-coated ZnO also has O–H stretching and C–O vibration bands, as well as C=O stretching, CH_2 bending, and C–N stretching due to adsorbed PVP. The frequency of the C=O stretching shifted from 1649 cm^{-1} in PVP to 1665 cm^{-1} in PVP-coated ZnO. This shift is indicative of chemical adsorption of PVP onto the ZnO surface through the carbonyl oxygen ligand [21]. Such interaction between zinc and carbonyl oxygen could explain the suppression of O=C=O stretching (Peak 6) in PVP-coated ZnO. The carbonyl oxygen ligands from PVP possibly attached to the exposed zinc ions at the ZnO surface and prevented the zinc ions from interacting with atmospheric CO_2.

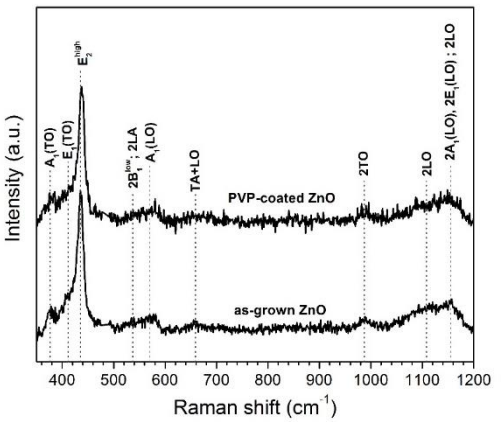

Figure 3. Raman spectra of as-grown and PVP-coated ZnO microrods.

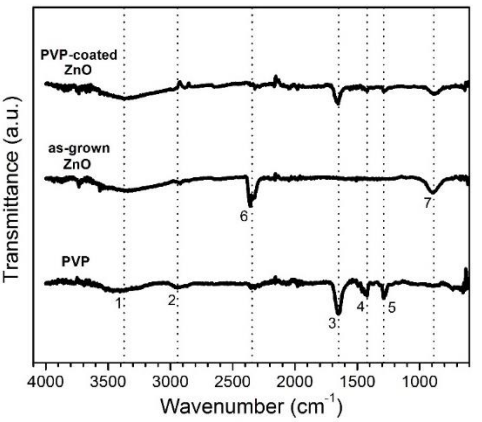

Figure 4. FTIR spectra of PVP as-grown ZnO and PVP-coated ZnO microrods

Figure 5 shows the room-temperature PL spectra of the as-grown ZnO and PVP-coated ZnO microrods. Both samples exhibit UV emission and visible emission due to near-band-edge and defect-related transitions, respectively. The defect emission intensity decreased and its peak shape changed after PVP coating. For the as-grown ZnO, the defect emission is a broad and asymmetrical peak. For the PVP-coated sample, the defect emission is resolved into two peaks. Figure 6 shows the Gaussian fitting of the PL spectra of the samples. The defect emission is decomposed to green and red emissions. Green emission is usually attributed to oxygen vacancies and surface defects [22-25]. On the other hand, red emission has been attributed to excess oxygen and defects related to zinc interstitials [5,24]. The intensities of green and red emission both decreased after PVP coating. Initially, the green emission is more intense than the red emission. Then, the green emission becomes less intense after coating. PVP coating suppressed green emission more effectively than the red emission.

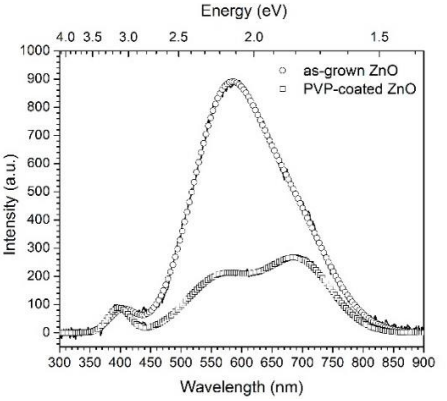

Figure 5. PL spectra of as-grown ZnO and PVP-coated ZnO microrods.

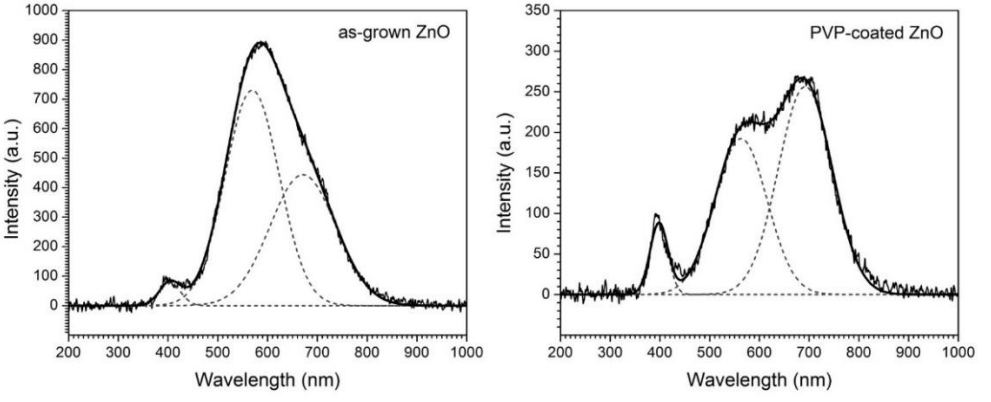

Figure 6. Gaussian fitting of the PL spectra of as-grown ZnO and PVP-coated ZnO microrods.

CONCLUSION

The defect emission of hydrothermally grown ZnO microrods consisted of a broad, asymmetrical peak. After coating with PVP, the defect emission was resolved into green and red emission bands. PVP coating also decreased the intensity of the defect emission and suppressed the green emission more effectively. Therefore, PVP can be used to alter the optical emission of ZnO and potentially target particular defect emissions.

ACKNOWLEDGMENT

This study is financially supported by the National Research Council of the Philippines (NRCP Project No. I-96). The authors would also like to thank the Earth Materials Science Laboratory (National Institute of Geological Sciences, University of the Philippines) and Sarukura Laboratory (Institute of Laser Engineering, Osaka University, Japan) for their services.

REFERENCES

1. Cho S, Ma J, Kim Y, Sun Y, Wong GKL, Ketterson JB. Photoluminescence and ultraviolet lasing of polycrystalline ZnO thin films prepared by the oxidation of the metallic Zn. Applied Physics Letters 1999;75:2761–3. doi:10.1063/1.125141.
2. Ding M, Zhao D, Yao B, E S, Guo Z, Zhang L, et al. The ultraviolet laser from individual ZnO microwire with quadrate cross section. Optics Express 2012;20:13657. doi:10.1364/oe.20.013657.
3. Reynolds D, Look D, Jogai B. Optically pumped ultraviolet lasing from ZnO. Solid State Communications 1996;99:873–5. doi:10.1016/0038-1098(96)00340-7.
4. Ryu YR, Lubguban JA, Lee TS, White HW, Jeong TS, Youn CJ, et al. Excitonic ultraviolet lasing in ZnO-based light emitting devices. Applied Physics Letters 2007;90:131115. doi:10.1063/1.2718516.
5. Djurišić AB, Leung YH, Tam KH, Ding L, Ge WK, Chen HY, et al. Green, yellow, and orange defect emission from ZnO nanostructures: Influence of excitation wavelength. Applied Physics Letters 2006;88:103107. doi:10.1063/1.2182096.
6. Baratto C, Kumar R, Comini E, Faglia G, Sberveglieri G. Visible electroluminescence from a ZnO nanowires/p-GaN heterojunction light emitting diode. Optics Express 2015;23:18937. doi:10.1364/oe.23.018937.
7. Moya MCB, Samantilleke A, Mollar M, Marí B. Nanostructured hybrid ZnO thin films for energy conversion. Nanoscale Research Letters 2011;6:384. doi:10.1186/1556-276x-6-384.
8. Pan Z-Y, Liang J, Zheng Z-Z, Wang H-H, Xiong H-M. The application of ZnO luminescent nanoparticles in labeling mice. Contrast Media & Molecular Imaging 2011;6:328–30. doi:10.1002/cmmi.434.
9. Kim SH, Umar A, Hahn Y-B, Al-Hajry A, Abaker M. Low-Temperature Growth of Aligned ZnO Nanorods: Effect of Annealing Gases on the Structural and Optical Properties. Journal of Nanoscience and Nanotechnology 2014;14:4564–9. doi:10.1166/jnn.2014.9029.
10. Mahmood A, Ahmed N, Raza Q, Khan TM, Mehmood M, Hassan MM, et al. Effect of thermal annealing on the structural and optical properties of ZnO thin films deposited by the reactive e-beam evaporation technique. Physica Scripta 2010;82:065801. doi:10.1088/0031-8949/82/06/065801.
11. Polydorou E, Zeniou A, Tsikritzis D, Soultati A, Sakellis I, Gardelis S, et al. Surface passivation effect by fluorine plasma treatment on ZnO for efficiency and lifetime improvement of inverted polymer solar cells. J Mater Chem A 2016;4:11844–58. doi:10.1039/c6ta03594a.
12. Meena JS, Chu M-C, Chang Y-C, You H-C, Singh R, Liu P-T, et al. Effect of oxygen plasma on the surface states of ZnO films used to produce thin-film transistors on soft plastic sheets. Journal of Materials Chemistry C 2013;1:6613. doi:10.1039/c3tc31320d.
13. Qin L, Shing C, Sawyer S, Dutta PS. Enhanced ultraviolet sensitivity of zinc oxide nanoparticle photoconductors by surface passivation. Optical Materials 2011;33:359–62. doi:10.1016/j.optmat.2010.09.020.

14. Liu KW, Chen R, Xing GZ, Wu T, Sun HD. Photoluminescence characteristics of high quality ZnO nanowires and its enhancement by polymer covering. Applied Physics Letters 2010;96:023111. doi:10.1063/1.3291106.
15. Kan C, Cai W, Li C, Zhang L. Optical studies of polyvinylpyrrolidone reduction effect on free and complex metal ions. Journal of Materials Research 2005;20:320–4. doi:10.1557/jmr.2005.0039.
16. Cuscó R, Alarcón-Lladó E, Ibáñez J, Artús L, Jiménez J, Wang B, et al. Temperature dependence of Raman scattering inZnO. Physical Review B 2007;75. doi:10.1103/physrevb.75.165202.
17. Feng W, Tao H, Liu Y, Liu Y. Structure and optical behavior of nanocomposite hybrid films of well monodispersed ZnO nanoparticles into poly (vinylpyrrolidone). J Mater Sci Technol 2006:22:230-4. doi: 10.3321/j.issn:1005-0302.2006.02.018.
18. Sui X, Liu Y, Shao C, Liu Y, Xu C. Structural and photoluminescent properties of ZnO hexagonal nanoprisms synthesized by microemulsion with polyvinyl pyrrolidone served as surfactant and passivant. Chemical Physics Letters 2006;424:340–4. doi:10.1016/j.cplett.2006.04.053.
19. Du T, Ilegbusi OJ. Synthesis and morphological characterization on PVP/ZnO nano hybrid films. Journal of Materials Science 2004;39:6105–9. doi:10.1023/b:jmsc.0000041712.35581.4c.
20. Chithra MJ, Sathya M, Pushpanathan K. Effect of pH on Crystal Size and Photoluminescence Property of ZnO Nanoparticles Prepared by Chemical Precipitation Method. Acta Metallurgica Sinica (English Letters) 2015;28:394–404. doi:10.1007/s40195-015-0218-8.
21. Jukić M, Sviben I, Zorić Z, Milardović S. Effect of Polyvinylpyrrolidone on the Formation AgBr Grains in Gelatine Media. Croatica Chemica Acta 2012;85:269–76. doi:10.5562/cca1919.
22. Ong H, Du G. The evolution of defect emissions in oxygen-deficient and -surplus ZnO thin films: the implication of different growth modes. Journal of Crystal Growth 2004;265:471–5. doi:10.1016/j.jcrysgro.2004.02.010.
23. Yao B, Feng L, Cheng C, Loy MMT, Wang N. Tailoring the luminescence emission of ZnO nanostructures by hydrothermal post-treatment in water. Applied Physics Letters 2010;96:223105. doi:10.1063/1.3443636.
24. Fabbri F, Villani M, Catellani A, Calzolari A, Cicero G, Calestani D, et al. Zn vacancy induced green luminescence on non-polar surfaces in ZnO nanostructures. Scientific Reports 2014;4. doi:10.1038/srep05158.
25. Gomi M, Oohira N, Ozaki K, Koyano M. Photoluminescent and Structural Properties of Precipitated ZnO Fine Particles. Japanese Journal of Applied Physics 2003;42:481–5. doi:10.1143/jjap.42.481.